A High-performance Echelle Grating De-multiplexer Based on Two Stigmatic Points and Its Flat-top Solution

Y. Zhang *, M. Schneider, D. Karnick, L. Eisenblätter, T. Kühner, M. Weber
Karlsruhe Institute of Technology, Institute for Data Processing and Electronics,
Hermann-von-Helmholtz-Platz 1, 76344 Eggenstein-Leopoldshafen, Germany

ABSTRACT

A wavelength filter is a key component for numerous photonic integrated circuit applications in optical communication. Researchers put forward several methods to design wavelength filters for which the Echelle grating de-multiplexers (EG-DMUXs) are popular and have been extensively studied.

In comparison with the traditional EG-DMUXs based on the Rowland mounting, EG-DMUXs based on the two stigmatic points (TSP) method were reported rather late. This paper will present the basic design theory and a high-performance device fabricated on a 250 nm silicon-on-insulator (SOI) platform for validation. The simulation and measurement results of this 1×7 EG-DMUX with 800 GHz channel spacing will be presented and compared. Although the fabricated device has the merits of compact on-chip footprint, low insertion loss and low crosstalk, its narrow 1-dB bandwidth may limit its application in practice. We present our solution to widen the transmission spectrum based on the TSP EG-DMUXs and multimode interferometers.

Keywords: Echelle grating, de-multiplexer, wavelength division multiplexing (WMD), silicon on insulator (SOI), flat-top.

1. INTRODUCTION

With a developing fabrication technology for photonic components on SOI, integrating more and more complex systems on chip becomes feasible. In the past decade, there were numerous publications reporting on the research progress of individual components including fiber-chip coupling components [1], power splitters and combiners [2], modulators [3], wavelength filters [4],[5] and many more. As key components for a system on chip, researchers have proposed several different methods to design wavelength filters, where the popular ones are arrayed waveguide gratings (AWGs) [6], ring resonators [7], lattice-form filters [8] and Echelle gratings [9]. Compared to the other three methods, the Echelle grating has the merits of compact on-chip size and weak sensitivity to local process variations, therefore it is widely studied. Among the publications on Echelle grating de-multiplexers, the Rowland circle method [10] is reported and studied most. Whereas, another design method based on two stigmatic points [11] is becoming more attractive since the advanced fabrication technology today makes fabricating more complex and tiny grating elements feasible. In this paper, a basic design theory of Echelle gratings based on two stigmatic points is presented and validated by a fabricated high-performance device. To further widen the transmission spectrum, multimode interferometers are adopted in the design to achieve flat-top response and the simulation result of three designed devices are presented.

2. TWO STIGMATIC POINT METHOD

The important property of ellipses used in the two stigmatic point method is that the sum of path lengths between a random point on the ellipse to one focus and to the other focus is constant. On this basis, the problem of designing an Echelle grating can be simplified by regarding the input and output channels as several focal points and selecting two pairs of them. The first pair is made up of the input point O and one output point F_1 and the other pair is made up of the input point O and another output point F_2 as shown in Figure 1. In our design model, the two outer-most output channels are used as focuses F_1 and F_2.

Incident light with wavelength λ_1 should be filtered to output channel F_1 and light with wavelength λ_2 should be filtered to output channel F_2. The effective wavelength in the guiding material for the two wavelengths are λ_{eff1} and λ_{eff2}, respectively. Then, one can draw a set of ellipses regarding the first pair of focuses O and F_1, and the corresponding constant path

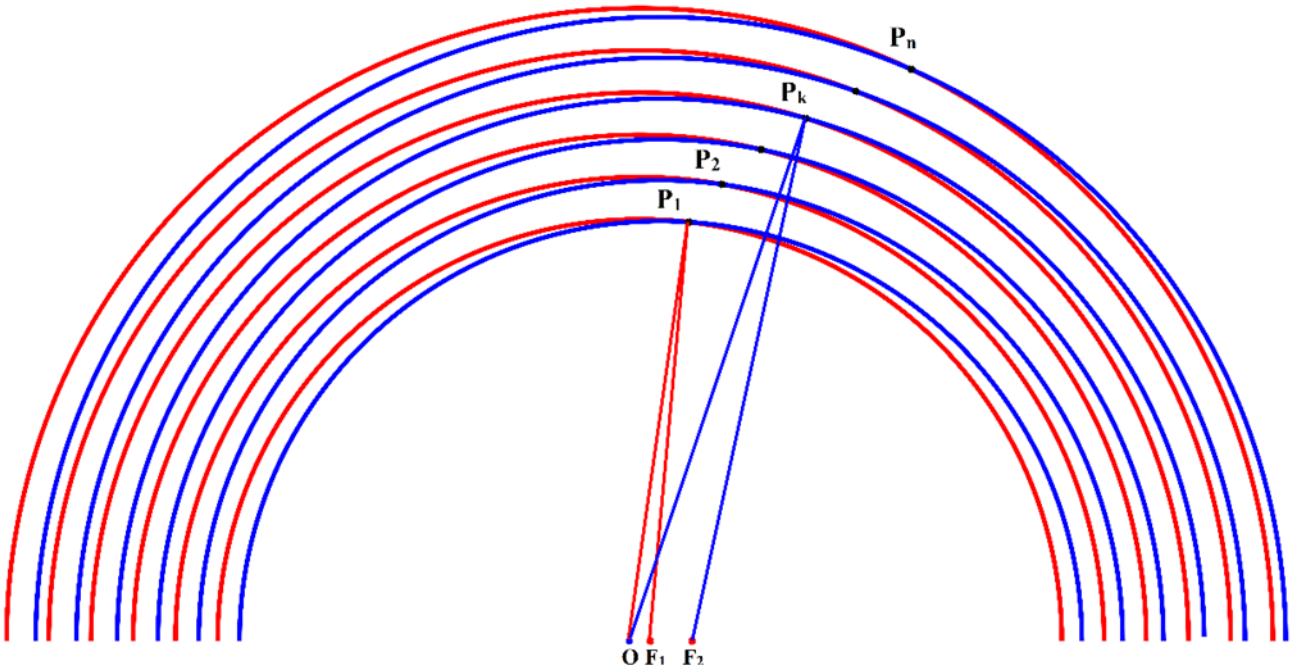

Figure 1. Diagram of the construction of Echelle grating demultiplexer with two stigmatic points.

$a_1 = \lambda_{eff1} \times m \times N_k$, where the parameter m is the diffraction order and N_k is a random integer. In the same way, a second set of ellipses can be drawn regarding the other pair of focuses, O and F_2, and the corresponding constant path $a_2 = \lambda_{eff2} \times m \times N_k$. Two sets of ellipses will generate a series of intersections P_1, P_2, ⋯, P_k, ⋯, P_n. The resulting path relations are shown in Table 1. Since N_1, N_2, ⋯, N_k, ⋯ N_n and m are all integers, the phase difference between any optical path $|\overrightarrow{OP_k}| + |\overrightarrow{P_kF_1}|$ should be an integer multiple of 2π, i.e. constructive interference takes place at output point F_1 for light with wavelength λ_1. In the same way, constructive interference takes place at output point F_2 for light with wavelength λ_2. Therefore, light with a different wavelength is filtered to its corresponding channel.

According to the analysis above, grating points also the coordinates for the reflectors, are the intersections P_1, P_2, ⋯, P_k, ⋯, P_n. In our design, Bragg reflector elements are used and each element is made up of 4 parallel reflectors with a depth of 160 nm and a center-to-center distance of 320 nm. Each reflector element is rotated so that light is reflected to the desired channels.

Table 1. The path relations of two sets of drawn ellipses.

$\|\overrightarrow{OP_1}\| + \|\overrightarrow{P_1F_1}\| = \lambda_{eff1} \times m \times N_1$	$\|\overrightarrow{OP_1}\| + \|\overrightarrow{P_1F_2}\| = \lambda_{eff2} \times m \times N_1$
⋯	⋯
$\|\overrightarrow{OP_k}\| + \|\overrightarrow{P_kF_1}\| = \lambda_{eff1} \times m \times N_k$	$\|\overrightarrow{OP_k}\| + \|\overrightarrow{P_kF_2}\| = \lambda_{eff2} \times m \times N_k$
⋯	⋯
$\|\overrightarrow{OP_n}\| + \|\overrightarrow{P_nF_1}\| = \lambda_{eff1} \times m \times N_n$	$\|\overrightarrow{OP_n}\| + \|\overrightarrow{P_nF_2}\| = \lambda_{eff2} \times m \times N_n$

3. AN 800 GHZ ECHELLE GRATING DE-MULTIPLEXER

We developed a customized design kit [9] in Matlab, based on the above method. All key parameters are used as input arguments to generate an Echelle grating layout. The generated layout can be exported as a GDS layout file as well as a simulation model for COMSOL Multiphysics.

The performance and footprint of the Echelle grating is highly determined by the grating span. To decrease the grating span while keeping a proper illumination of the grating, the divergence of light from the input channel into the free space region has to be narrowed. To this end, we tapered the access single-mode waveguides from 0.5 µm to 2 µm over a length of 30 µm and under the assumption of TE-polarized incident light. Using our self-developed kit, we designed and obtained a layout of a 1×7 Echelle grating de-multiplexer with a channel spacing of 800 GHz. The distances between O, F_1 and F_2 are $\left|\overrightarrow{OF_1}\right|$ = 9 µm and $\left|\overrightarrow{OF_2}\right|$ = 39.8 µm, respectively, the diffraction order is m = 9. For the calculation of the required

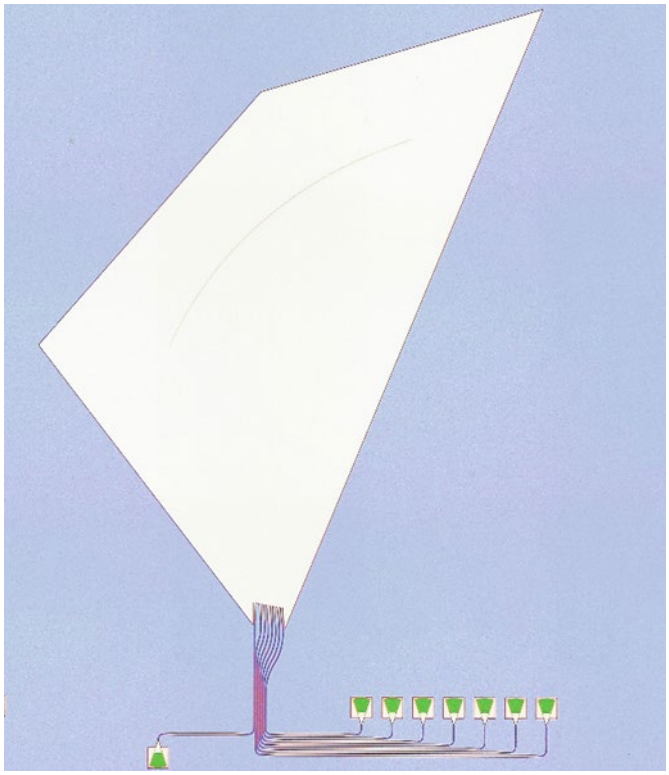

Figure 2. Microscope picture of the fabricated Echelle grating de-multiplexer.

grating points P_n, we defined the range of path lengths a_1 and a_2 to be between 398 µm and 716 µm. The designed device was fabricated on a 250 nm SOI platform and Figure 2 shows a microscope picture of the fabricated device. The white space is the free propagation region and the dark arc in the upper free propagation region is the Echelle gratings. Each I/O channel is connected to an out-of-plane grating coupler (green) at the bottom. This device has a grating span of 36.8° and an on-chip footprint of about 680 µm × 360 µm without taking the grating couplers and waveguides into account.

For the characterization, we used a tuneable laser to generate continuous-wave light in the C band. TE polarization of the incident light is ensured by a polarization controller. At the receiver side, an optical power meter (Agilent 81618A with 81623B detector head) is used to detect the output light.

The numerical simulations were conducted on a computer with 48 cores and 1 TB RAM. Both the simulated (dotted lines) and the measured (full lines) transmission spectra are illustrated in Figure 3. As can be seen, there is good agreement between the theoretical and experimental results in terms of the peak transmission of each channel. This device has an average transmission of -2.45 dB while the maximum transmission is -1.61 dB and the minimum transmission is -3.18 dB. The average crosstalk is -22.81 dB with a maximum value of -20.26 dB and a minimum value of -37.69 dB. The average

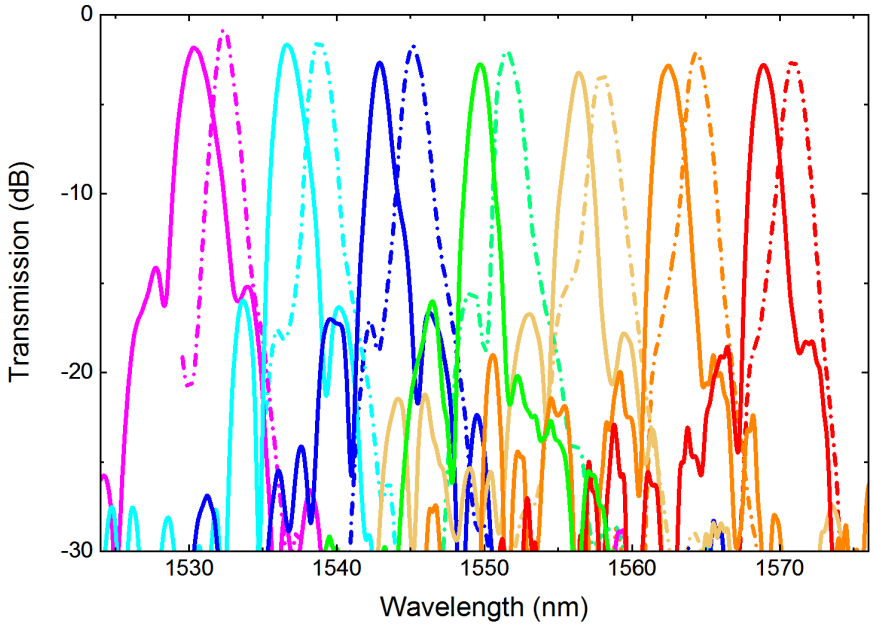

Figure 3. Measured and simulated transmission spectrum of the designed device.

1 dB-bandwidths is around 0.44 nm according to the curve fittings of the transmission peaks. Additionally, the measured spectrum has a blue shift of around 2 nm compared to the simulated spectrum due to a refractive index error. A possible reason is a deviation of the thickness of the silicon crystalline layer from the ideal value.

4. FLAT-TOP ECHELLE GRATING DE-MULTIPLEXERS

The narrow 1 dB-bandwidth of the device can be inconvenient to use in practice since its optimum operating wavelength can be easily affected by factors like fabrication quality, wafer quality, temperature etc.. To improve its wavelength shift tolerance, the transmission spectrum should be widened. To this end, we use multimode interferometers (MMI) to generate a flat input field instead of a Gaussian-like field to achieve a flattened spectral response.

Figure 4 shows the schematic of an MMI aperture used as the input channel of the Echelle grating de-multiplexer. The single mode input field of the MMI originates from a taper. The end of the taper has a width of w and is centered on the left side of the multimode region. The multimode region of the MMI has a width of W_{mmi} and a length of L_{mmi}. According to the self-imaging theory of MMIs [12], the first two-fold images will be presented at the position of $L = 3\pi/8(\beta_0 - \beta_1)$, where β_0 and β_1 are the propagation constants of the two lowest order modes. To make the design compact, a small W_{mmi} is required. Taking this into account, we selected the values 4 µm, 5 µm and 6 µm for W_{mmi}. Based on numerical

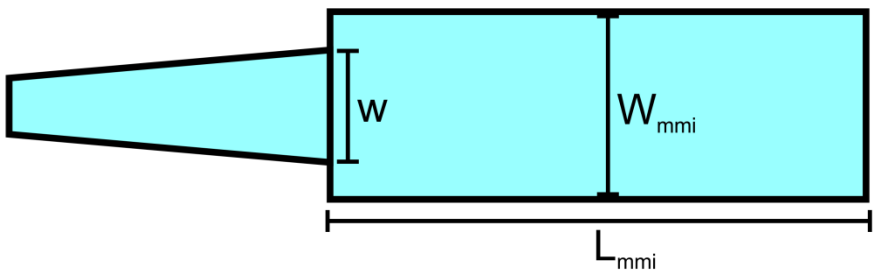

Figure 4. Schematic of an MMI.

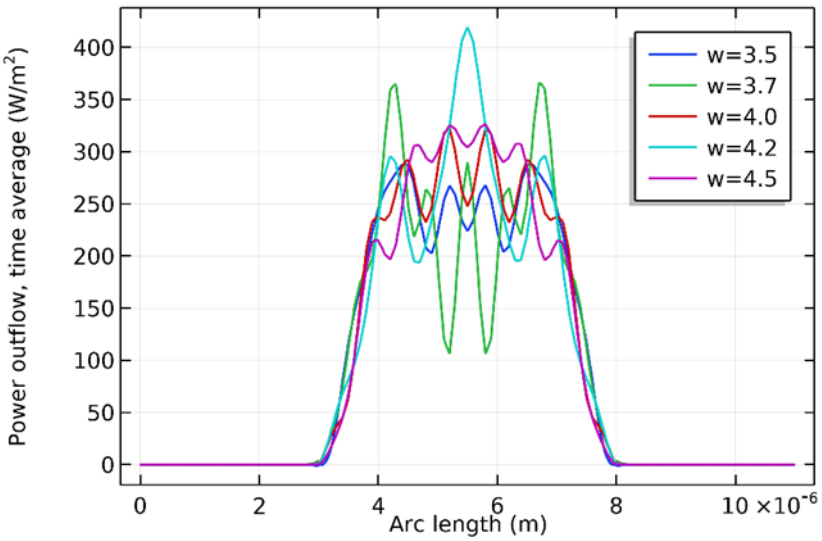

Figure 5. Mode field distribution at the end of an MMI for different input taper widths w.

simulations, the corresponding 2-fold imaging length of the MMIs are 14.5 µm, 22.8 µm and 33 µm, respectively. Since the overlap of two images determines the required flat field, their field profile and the distance between two fields' centres can affect the flatten response. Figure 5 shows the field distributions at the output end of an MMI with W_{mmi} = 5 µm and L_{mmi} = 22.8 µm. The output field is most flattened for a taper width of w = 3.5 µm. In a similar way, the parameter w for MMIs with W_{mmi} = 4 µm and W_{mmi} = 6 µm can be determined as well and are 3 µm and 4.7 µm, respectively.

Based on the above calculations, flat-top Echelle grating de-multiplexers can be designed by replacing the input access waveguide with the calculated MMIs. Keeping the design parameters of the Echelle grating de-multiplexers the same as the one presented in section 3 and using the three abovementioned MMIs, we obtain three flat-top designs. The numerical simulation results of the three devices are shown in Figure 6, Figure 7 and Figure 8, respectively. Among the three designs, the device with W_{mmi} = 6 µm (Figure 6) shows the best flat-top response with an average insertion loss of 5.25 dB. Compared to the simulation result shown in section 3, there is 2.7 dB penalty from the flat-top response. On the other hand,

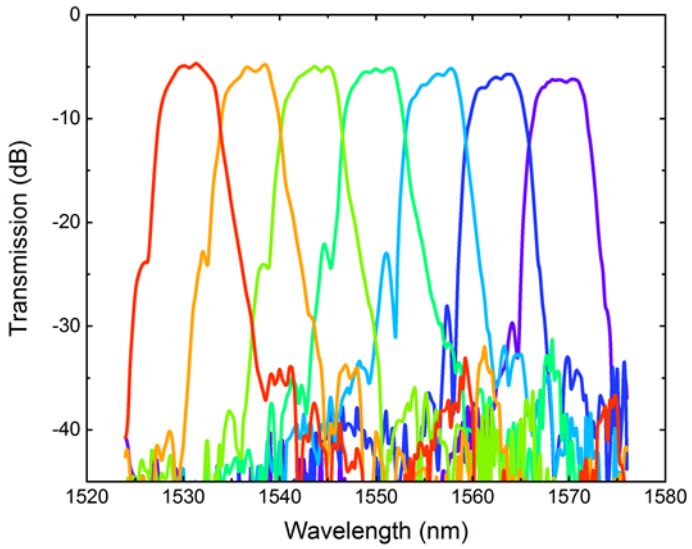

Figure 6. Transmission spectrum of a flat-top Echelle grating de-multiplexer with W_{mmi} = 6 µm.

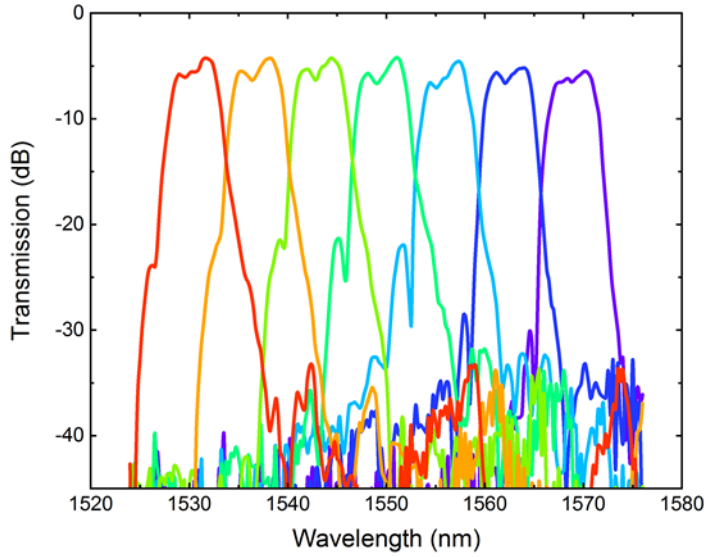

Figure 7. Transmission spectrum of a flat-top Echelle grating de-multiplexer with W_{mmi} = 5 µm.

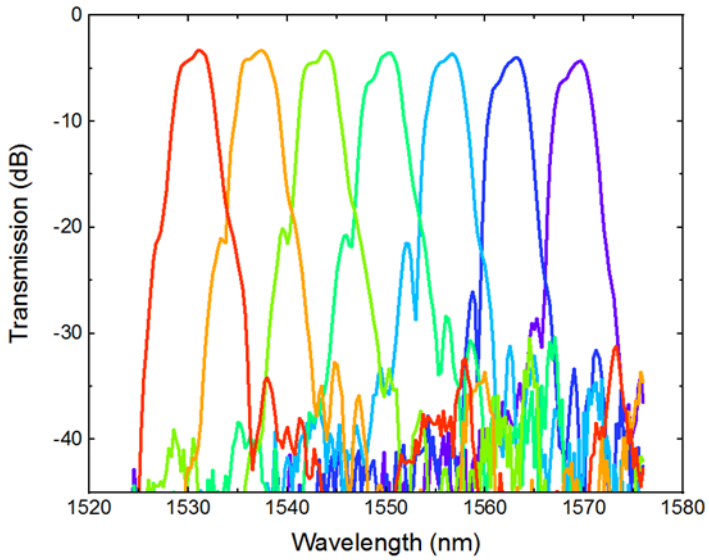

Figure 8. Transmission spectrum of a flat-top Echelle grating de-multiplexer with W_{mmi} = 4 µm.

the derived 1 dB-bandwidth is around 3 nm instead of 0.44 nm. The crosstalk remains similar with an average value of -23.74 dB. The average insertion loss of the other two devices increases with narrowing the width of the MMI, they are xxx dB (W_{mmi} = 5 µm) and xxx dB (W_{mmi} = 4 µm), respectively. Since the fluctuation of the transmission peak becomes stronger for smaller W_{mmi}, it is difficult to derive accurate 1-dB bandwidth for devices with W_{mmi} = 5 µm and W_{mmi} = 4 µm. Nevertheless, one can observe the tendency of flattened peak in comparison with the spectrum shown in Figure 3.

As can be seen, the transmission spectrum can be flattened significantly at the price of higher insertion loss. Therefore one has to make a trade-off between insertion loss and bandwidth.

5. CONCLUSION

Based on the two stigmatic points design method, we designed and fabricated a compact 1×7 EG-DMUX with an on-chip footprint of 680 μm × 360 μm. Its simulation and measurement results show an excellent agreement where the measured average insertion loss is 2.45 dB, the average crosstalk -22.81 dB, and the 1 dB-bandwidth 0.44 nm. To increase the 1 dB-bandwidth, we use an MMI at the input channel to achieve a flat-top response. In our proposed designs, the device with a multimode region width of 6 μm presents the best flat-top response with the 1-dB bandwidth being increased to 3 nm. Simultaneously, the average insertion loss is increased to 5.25 dB. Further investigation is still required to improve the 1-dB bandwidth without increasing the insertion loss significantly.

6. ACKNOWLEDGEMENT

This research is supported by the program Matter and Technology of the Helmholtz Association, Germany and the China Scholarship Council (CSC), China.

REFERENCES

[1] Chen X, Tsang HK. "Polarization-independent grating couplers for silicon-on-insulator nanophotonic waveguides." Optics letters 36.6 (2011): 796-798.

[2] Ren F, Chen W, Zhangsun T, Zhang Y, Fan X, Wang J. "Variable-ratio mode-insensitive 1×2 power splitter based on MMI couplers and phase shifters." IEEE Photonics Journal 10.5 (2018): 1-12.

[3] Marris-Morini D, Baudot C, Fédéli JM, Rasigade G, Vulliet N, Souhaité A, Ziebell M, Rivallin P, Olivier S, Crozat P, Le Roux X. "Low loss 40 Gbit/s silicon modulator based on interleaved junctions and fabricated on 300 mm SOI wafers." Optics express 21.19 (2013): 22471-22475.

[4] Sciancalepore C, Lycett RJ, Dallery JA, Pauliac S, Hassan K, Harduin J, Duprez H, Weidenmueller U, Gallagher DF, Menezo S, Bakir BB. "Low-crosstalk fabrication-insensitive echelle grating demultiplexers on silicon-on-insulator." IEEE Photonics Technology Letters 27.5 (2014): 494-497.

[5] Zhang Y, Schneider M, Karnick D, Eisenblätter L, Kühner T, Weber M. "Key building blocks of a silicon photonic integrated transmitter for future detector instrumentation." Journal of Instrumentation 14.08 (2019): P08021.

[6] Castellan C, Tondini S, Mancinelli M, Kopp C, Pavesi L. "Low crosstalk silicon arrayed waveguide gratings for on-chip optical multiplexing." Silicon Photonics: From Fundamental Research to Manufacturing. Vol. 10686. International Society for Optics and Photonics (2018): DOI: 10.1117/12.2306120.

[7] Zheng S, Cai H, Gu YD, Chin LK, Liu AQ. "High-resolution on-chip spectrometer with a tunable micro-ring resonator filter." 2016 Conference on Lasers and Electro-Optics (CLEO). IEEE (2016): AM1J.2.

[8] Horst F, Green WM, Assefa S, Shank SM, Vlasov YA, Offrein BJ. "Cascaded Mach-Zehnder wavelength filters in silicon photonics for low loss and flat pass-band WDM (de-) multiplexing." Optics express 21.10 (2013): 11652-11658.

[9] Zhang Y, Schneider M, Karnick D, Eisenblätter L, Kühner T, Weber M. "Low-loss and robust DWDM Echelle grating (de-) multiplexers in SOI technology." Optical Components and Materials XVI. Vol. 10914. International Society for Optics and Photonics (2019): DOI: 10.1117/12.2507433.

[10] Lycett RJ, Gallagher DF, Brulis VJ. "Perfect chirped echelle grating wavelength multiplexor: design and optimization." IEEE Photonics Journal 5.2 (2013): 2400123-2400123.

[11] Horst F, Green WM, Offrein BJ, Vlasov Y. "Echelle grating WDM (de-) multiplexers in SOI technology, based on a design with two stigmatic points." Silicon Photonics and Photonic Integrated Circuits. Vol. 6996. International Society for Optics and Photonics (2008): DOI: 10.1117/12.781232.

[12] Bryngdahl O. "Image formation using self-imaging techniques." JOSA 63.4 (1973): 416-419.